

# **LAPS - Laser Aided Powder Solidification - Technology for the direct production of metallic and polymer parts**

P. Eyerer, J. Shen, B. Keller

Institute of Polymer Testing and Polymer Science , Department  
of Polymer Engineering, IKP - University of Stuttgart,  
Pfaffenwaldring 32, 70569 Stuttgart, FRG

## **Abstract**

The prototypes of today's commercial available RP-Systems (e.g. Stereolithography-Systems) are suitable mainly for designing and, if even, for restricted functional tests. From this it can be concluded that for obtaining functional or technical prototypes one has to use time- and cost-intensive downstream-technologies like investment casting. Because of the economical aspects in industries there is a great demand for direct production of functional and technical prototypes.

The present paper describes the activities and research results on the development techniques based on laser induced solidification of powder materials for the direct manufacturing of metallic parts. Also a various number of polymers, suitable for sintering and remelting, are investigated and presented as functional materials for different applications.

## **1. Introduction**

The technics of Laser Aided Powder Solidification have been used to generate metallic and polymer parts. Analogous to the technics of laser surface treatment, the powder is preplaced onto a substrate and melted or sintered within the laser irradiated zone [1]. The part will be built up with the principle of the well-known Layer Manufacturing Technology (LMT).

With regard to the metal powder application a number of copper-based powder mixtures with different weight percentages of lead and tin were investigated. In this case of applying a mixture of high and low melting materials, a sintering process will be accelerated by generating a liquid phase [2,3]. Therefore the processing temperature, caused by the energy coupling of the laser beam, has to be between both melting points. According to the experimental results described below it is generally necessary to keep the liquid phase as long as possible, because its surface tension will provide the driving force for sintering. Optimization due to the main processing parameters laser power  $P$ , beam intensity  $I$  and energy density  $H$  using the LAPS-testbed is carried out with respect to reduced curl distortion and better interlayer metallurgical bonding.

The LAPS laboratory equipment (low-power laser) is employed to perform optimization on polymer powder analogous to metal powders. Polystyrene and Polyamid-Copolymer are presented as suitable materials for plaster block mouldings and functional elastomeric parts, respectively.

## 2. Experimental procedure for metal powder mixtures

The laser used for our experiments is a cw (continuous wave) CO<sub>2</sub>-laser with a maximum output power of 1500 W (TLF1500). The laser beam has a gaussian intensity distribution and is focused with a parabolic copper mirror (focal length  $f=300\text{mm}$ ). The minimum of the achievable beam diameter is  $d_L=0.35\text{mm}$ . The test bed with ridgeless layer levelling for metal powder application is fixed onto a 3-axis CNC coordinate machine (figure 1). Although powder heating option was available, the experiments were carried out at room temperature in order to avoid bonding of the entire powder bed. Argon is used as protective gas in an open atmosphere.

The surface temperature of the partially sintered powder during laser processing is detected using an infrared pyrometer. This signal is employed for a closed loop control of the laser power and transformed into a temperature signal for the user control. Therefore a PID control system has been developed in order to transform the desired input signal of the measured temperature and a DC output signal for the direct transmitting control of the laser power. Additional to the pyrometric power control, temperature measurements with thermocouples in different heights of the layers and IR-temperature distribution on the powder surface with a thermography camera were performed.

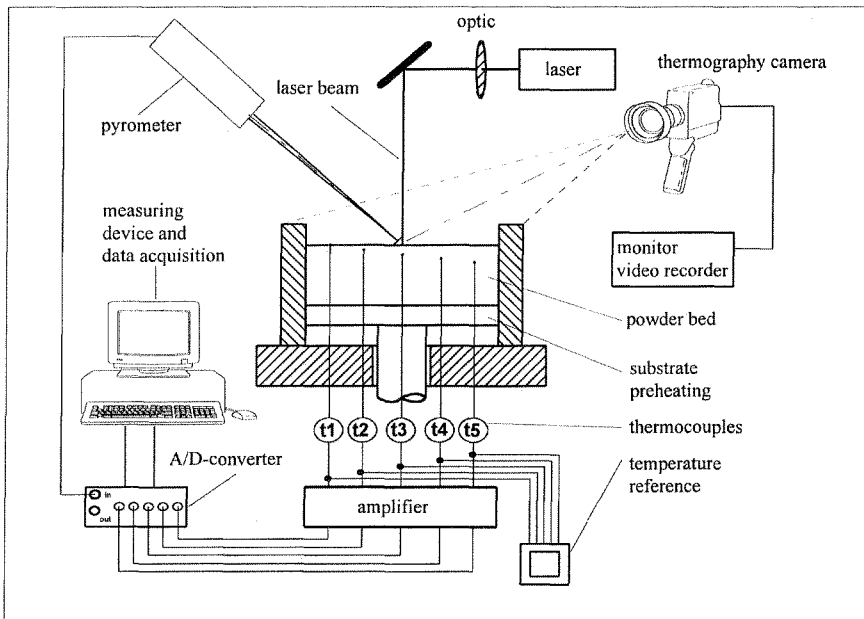


Fig. 1: Principle of on-line IR-temperature-measurement and pyrometric power control during the laser sintering process

All kinds of pulverulent materials used in the overall work are pure metals (Cu, Pb, Sn) or their mixtures (Cu mixed with 10, 20, 30 and 50 wt.-% Pb and Cu mixed with 5, 11, 15, 20 wt.-% Sn). Their particle size is less than  $45\ \mu\text{m}$  and the particle shape is chosen approximately spherical because of the good behaviour during the layer levelling.

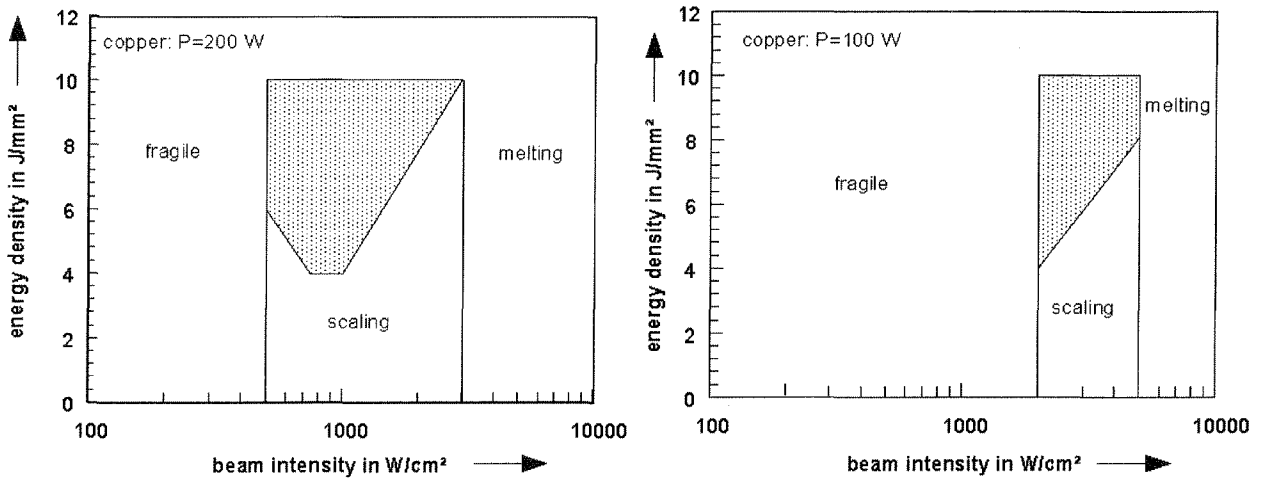
The representation of the results in this paper are focusing on pure copper and copper-lead mixture with 20 wt.-% lead addition but references in the conclusion are given also for other powder mixtures.

$$d_L = \sqrt{\frac{4 \cdot P}{\pi \cdot I}} \quad (1), \quad \text{and} \quad v = \frac{P}{H \cdot d_L} \quad (2).$$

To classify the results of laser sintering, the width and heights of each sintered track were measured and their strength and faults (oxidation, melting, scale like structure) were registered. Metallographic investigations (SEM and light microscopy) were carried out to get the information about the sintering progress and the microstructure of the sintered tracks.

## 2.1 Results on pure copper powder

During laser sintering pure copper powders should not be melted. At an elevated processing temperature the bond between the particles can only be established by means of activated diffusion process. A strong bond of the particles, respectively high strength and density, cannot be reached because of the limited interaction time (up to 1,5 s) of laser beam and powder bed.



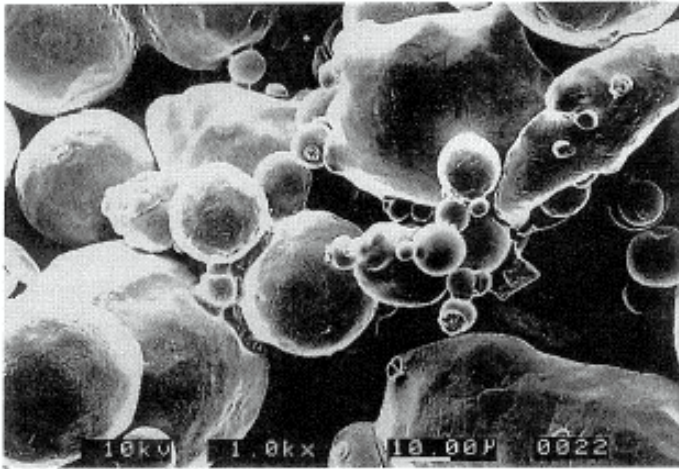
**Fig. 2 and 3:** Working area (hatched zone) of beam intensity and energy density for laser sintering of copper powder at P=200 W and P=100W

Fig. 2 and 3 show the working areas of energy density as function of beam intensity for different laser powers. Because of extremely short diffusion time the tracks sintered at beam intensities lower than 500 W/cm<sup>2</sup> are fragile. Higher beam intensity causes an increasing strength of the sintered tracks. Above I=3000 W/cm<sup>2</sup> the copper powder was molten and chains of metal balls were observed in the middle of the track.

Also the energy density affects the sintering process. In the low range of energy density ( $H \leq 4 \text{ J/mm}^2$ ) a scale-like structure occurs on the surface of the track. Because of the thermal tension and the weak powder bond at low energy densities, pieces of powder blocks (scales) rise from the powder bed. Experiments were done at energy densities up to 10 J/mm<sup>2</sup>. If the laser power is reduced from 200 W down to 100 W, the working area shifts to high values of beam intensity (comparing Fig. 2 to Fig. 3). A further reduction of

the laser power (at  $P=50\text{ W}$ ) results fragile sintered tracks at all investigated values of beam intensity and energy density.

Fig. 4 shows a cross sectional SEM micrograph of a sintered track. The bond of laser induced sintering necks between the powder particles is weak, but high enough for depositing from the powder bed (analogous to green part strength).



**Fig. 4:** Cross sectional SEM-micrograph of laser sintered copper powders, showing the sintering necks between powder particles. ( $P=100\text{ W}$ ,  $I=2000\text{ W/cm}^2$ ,  $H=8\text{ J/mm}^2$ )

The width and the height of laser sintered tracks are illustrated as a function of energy density and beam intensity in Fig.5 and 6. The working areas are hatched. With increasing energy density (though the beam diameter remains constant) the track width rises (Fig. 5). Under the given parameter combination ( $P=200\text{ W}$  and  $I=1000\text{ W/cm}^2$ ) good tracks can be produced only if energy density is more than  $4\text{ J/mm}^2$ . The broken line in Fig. 5 marks the layer thickness of the powder bed. Since the track width is linearly proportional to the beam diameter, it drops with increasing beam intensity (Fig. 6).

the beam diameter, it drops with increasing beam intensity (Fig. 6).

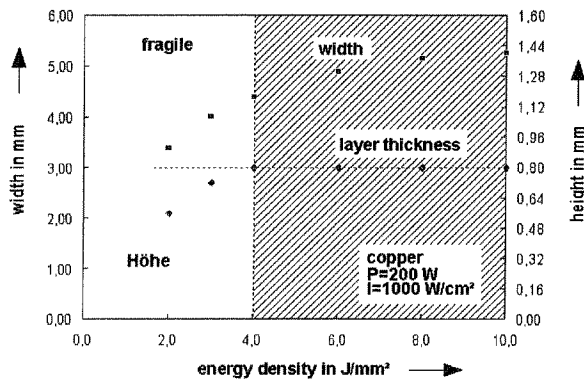


**Fig. 5:** Width and height of single tracks of copper as a function of the beam energy density. ( $P=200\text{ W}$ ,  $I=1000\text{ W/cm}^2$ )

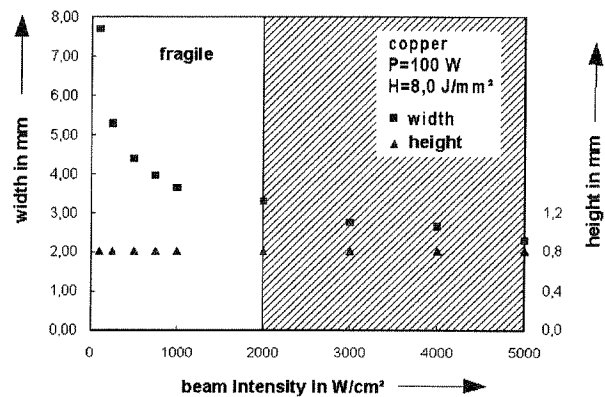


**Fig. 6:** Width and height of single tracks of copper as a function of the beam intensity. ( $P=100\text{ W}$ ,  $H=8\text{ J/mm}^2$ )

## 2.2 Results on copper-lead powder mixtures

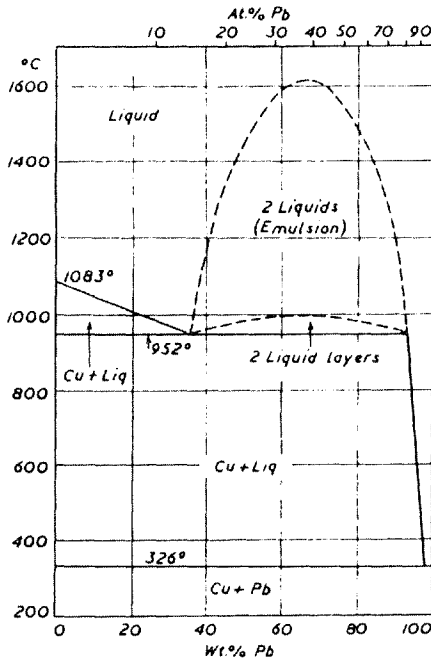


Fig. 7: Binary phase diagram of copper-lead [4]

Corresponding to the copper-lead binary phase diagram in fig. 7 lead does not dissolve in copper. Lead will be melted above  $T_m=326^\circ\text{C}$  and wets the copper particles. The requirements of liquid phase sintering are fulfilled if the processing temperature is kept below the melting point of copper ( $T_m=1083^\circ\text{C}$ ). It was determined, that an increasing content of lead results in an extending range of parameter variation and a further strengthening of the tracks compared to pure copper. With the minimum achievable constant laser power of  $P=50\text{ W}$  it was found that the intensity of  $I=50\text{ W/cm}^2$  is high enough for laser sintering Cu-Pb with 30 and even 20 wt.-% lead. However a further increase in lead addition (50 wt.-%) will lead to a strong narrowing of the working area. Fig. 7 shows the working area at  $P=100\text{ W}$  for Cu-Pb (20 wt.-%) and fig. 8 the corresponding width and heights of the sintered tracks as functions of the beam diameter.

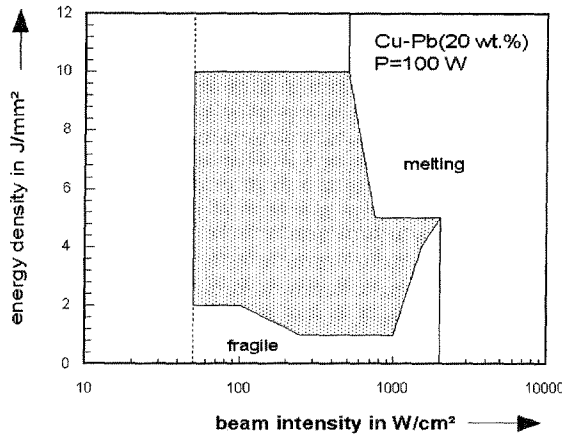


Fig. 7: The working area of laser sintering of CuPb 20 wt.-%.

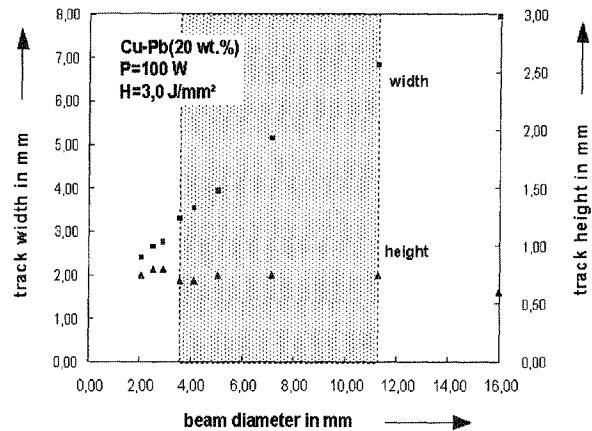
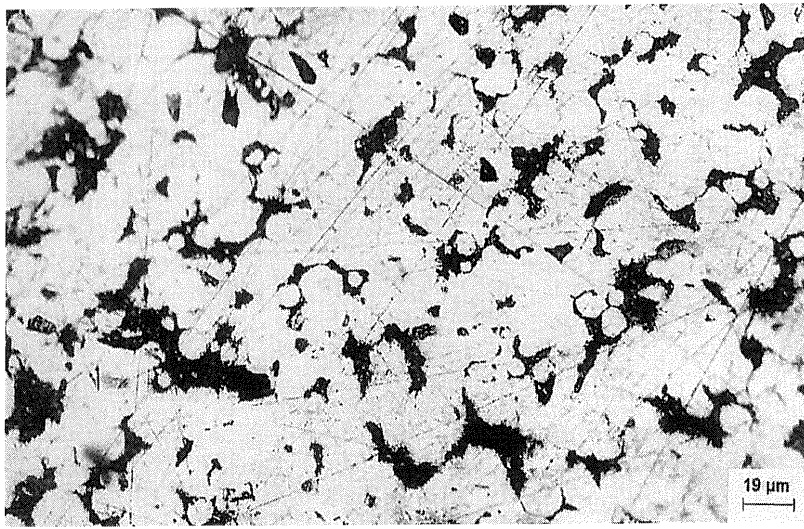


Fig. 8: Corresponding width and height of sintered tracks as function of beam diameter.

The relationship between track geometry and the processing parameters are quite similar to the sintering of pure copper powder (figs. 5 and 6). While the height remains almost constant, the track width rises linearly with increasing beam diameter (hatched zones refer to the working area).



**Fig. 9** Cross section of a sintered track (Cu + 20 wt.% Pb). (P=50 W, I=500 W/cm<sup>2</sup>, H=10 J/mm<sup>2</sup>)

In contrast to the laser sintering of pure copper powders the sintered tracks of copper-lead mixtures don't have the typical copper color. Fig. 9 is a micrograph of the cross section of a laser sintered track of Cu-Pb (20 wt.%). The color of the whole cross section is yellow, indicating that no pure copper powder particles exist anymore. The melted lead powder is distributed in the sintered track homogeneously. The porosity of the sintered track is lower than expected,

although the powders were not densified before laser sintering.

### 2.3 On-line measurement of temperature distribution

The experimental set-up of the temperature measurements in and on the powder bed is shown in figure 1. Specially fabricated Ni-CrNi thermocouples (0,2 mm thickness) covered with a glass layer were arranged in a line at different depths (0, 0.3, 0.6, 0.9 and 1.2 mm) in the powder bed (t1 to t5). Ceramic tubes were used for strengthening and electrical isolation. The laser irradiated zone was measured by the pyrometer and the temperature distribution on the powder surface was recorded by a thermography camera. Both surface temperature measurement devices were fixed constantly versus the laser beam axis. A special program for data acquisition and processing control was developed. These arrangements will allow the time- and point-disintegrated description of the process.

Quantitative optical temperature measurements require accurate data of emission degrees. They were measured by tailoring the optical devices repeatedly until the temperature measured with the thermocouple were identical. Pure copper showed an absorption rate of 30% and in case with lead addition they rise with increasing lead content, e.g. Cu-Pb (20 wt.-%) has an emission degree of 40%.

#### *Temperature distribution in the powder bed*

By modifying the temperature-time curves, derived from the thermocouples, one may get isotherms in the x-z-plane. The derived temperature maintaining time ( time interval, where the temperature is kept above the isotherm) enables the quantitative estimation of the sintering progress. In our case a liquid phase sintering is only possible if the processing temperature is at least T=326°C (fig.7). Considering the fast heating speed a isotherm of 350°C is chosen. Figure 10 describes the influence of lead content in the

powder mixture on the 350°C-isotherm. The respective temperature maintaining time is depicted in figure 11.

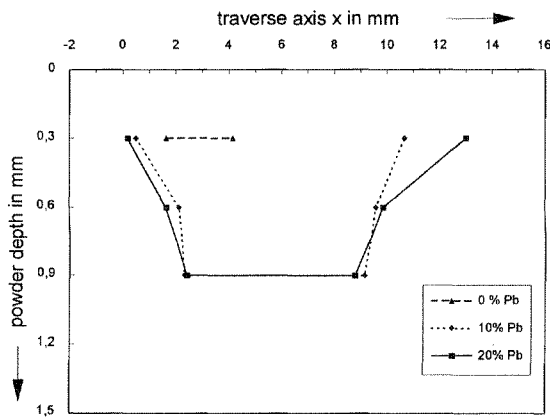


**Figure 10:** 350 °C isotherms of CuPb powder mixtures. Processing parameters:  $P=50W$ ;  $I = 500 \text{ W/cm}^2$ ;  $H = 6 \text{ J/mm}^2$

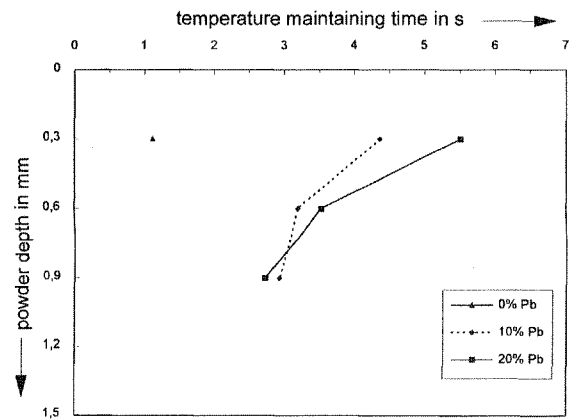


**Figure 11:** Corresponding temperature maintaining time of CuPb powder mixtures to fig. 10.

The 350°C isotherm of the pure copper powder occurs only at 0.3 mm under the powder surface. Temperature maintaining time is about 1 sec. If 10 or 20 wt.% lead is added into the powder the 350°C isotherm reaches a powder depth of 0.9 mm. A significant increase of the temperature maintaining time is observed respectively (figure 10 and 11).

Solid copper has a very poor absorption rate of the CO<sub>2</sub> laser beam. It is about 0.5 % for opaque surfaces. In shape of powder with the applied grain size it rises to a value of about 38% due to increasing surface of powder particles [5]. From the measurements of emission degree we know, that the absorption rate of Cu-Pb (20 wt.-%) powder mixture is about 50% higher than that of pure copper powder. It means that at the same processing parameters the CO<sub>2</sub> laser beam energy coupling of CuPb(20 wt.-%)-powder is about 50% more than of pure copper powder.

It seems the difference of energy coupling is clearly more than 50%. In fact copper-lead powder mixture has a lower thermal conductivity than the pure copper powder ( $\lambda_{Cu} = 384 \text{ W/mK}$ ,  $\lambda_{Pb} = 34,7 \text{ W/mK}$ ). A large part of the laser energy coupled into copper powder is conducted away from the processing area. In the case of Cu-Pb powder mixture heat flow into the powder bed is much lower. The laser heating is more "locally". This explains the larger isotherm area and longer temperature maintaining time

#### *Temperature distribution of the powder bed surface*

These investigation were performed for various relevant situations, e.g. single and rectangular tracks, overlappings and overhangings for different layer thicknesses. The results will help describing and understanding the sintering process. Following two figures show some results of Cu-Pb (20 wt.-%), which were received from a rectangular

contour at a corner and the comparison of the surface temperature before and during overlapping.

Figure 12a to 12c represent the temperature distribution at the first corner (1s delay to each other). Although the laser beam stays briefly at the corner (ca. 200ms) while reading a new NC-sentence, neither significant temperature increase nor shift of the distribution was observed.

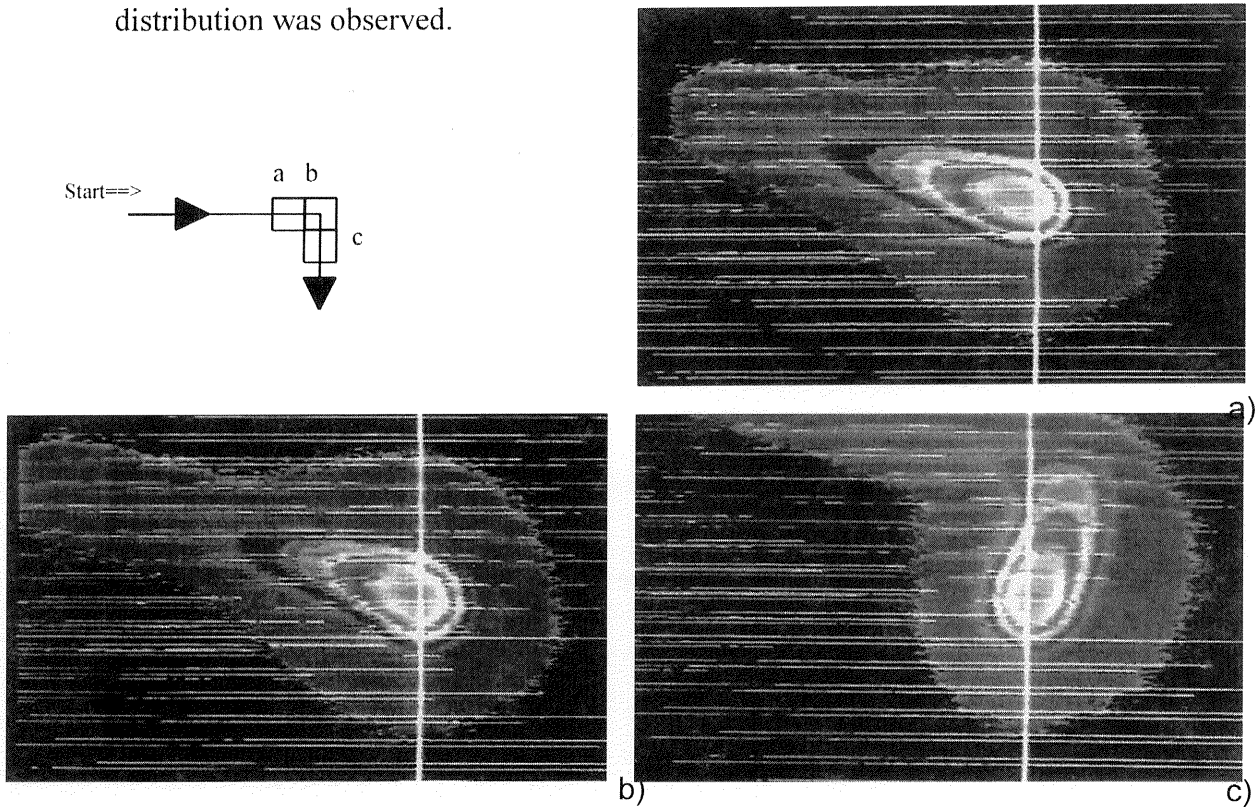
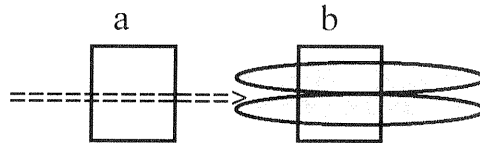


Figure 12: Surface temperature distribution during sintering process. Picture a, b and c have a delay of 1sec. Beam-powder interaction time is 1.5sec.

Figure 13 a and b describe the surface temperature at overlapping a new track on two already sintered tracks (powder depth is 1.2mm). Two effects are evident: the max. temperature in 13 a is is about 70°C higher than in 13 b and the elevated zone behind the laser beam is wider than in 13 b. This behaviour indicates a strong heat flow to the sintered region below. It is comprehensible because in the sintered region the molten lead wets the copper particles and increases the thermal conductivity.





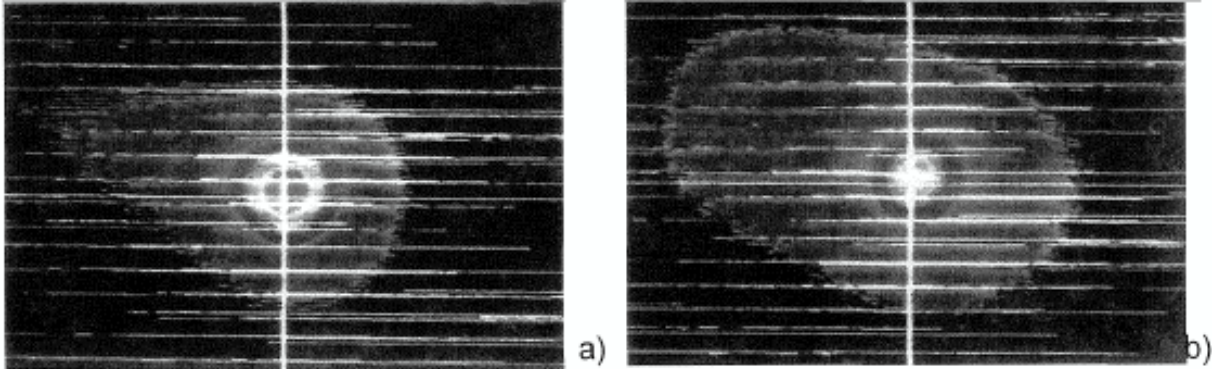


Figure 13: Surface temperature of overlapping a new laser sintering track on two sintered tracks. a) before overlapping,  $T_{\max.} = 563 \text{ }^\circ\text{C}$ ; b) during overlapping,  $T_{\max.} = 493 \text{ }^\circ\text{C}$ .

### 3. Experimental set-up on polymer powders

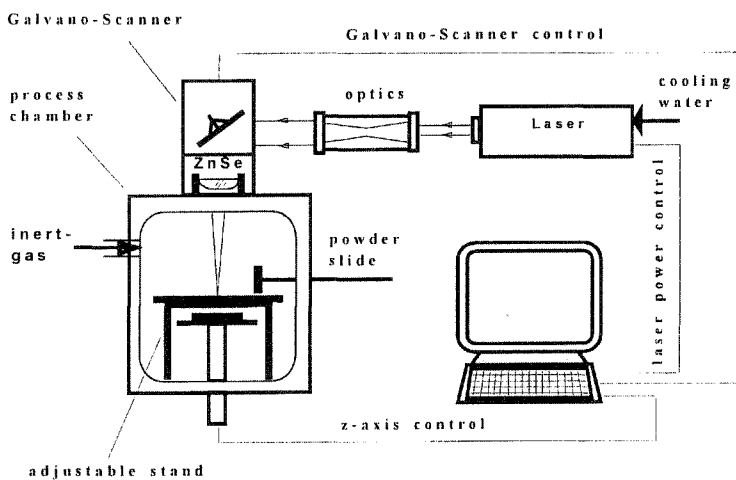


Figure 14: LAPS-laboratory equipment

The LAPS laboratory equipment is assembled consisting of a 50W CO<sub>2</sub>-laser, beam recess optics, high speed Galvano-Scanner, ZnSe-focus lense and a temperature controlled ( $T_{\max}=300^\circ\text{C}$ ) process-chamber with a ridgeless layer-levelling. The laser power, beam-movement and z-axis are software-controlled. This equipment has been acquired because of its suitability for polymers as well as for metal powders.

#### *Material selection*

The selection of polymer materials for our investigations was made in respect to the most employed technical thermoplasts in industries like PA, PE, PP, PVC, PS, ABS, PC and their compatible blends or bimodal powder mixtures. Although comprehensive investigations on these powders, especially for PA 11, showed satisfactory results referring to the layerwise build-up of complex parts, they are mostly employed for designing and restricted functional tests after postprocessing (infiltration and/or surface finish). However the main application have skilled metal prototypes via investment casting. Polystyrene polymer powder as RP-pattern after laser sintering is investigated for

use of a lost pattern for direct investment casting and elastomeric modified Polyamid as functional prototype.

### 3.1 Parameter optimization

The parameter optimization in respect to the polymer powders described below is done in a similar methodical technique as for metal powders but using laser sintered panels with the dimensions of 20mm x 20mm. The assumptions for defining optimal process parameters for working areas (energy density, beam intensity, hatching distance) were taken due to reduced curl distortion, rate of makroskopical sintering (strength of panel), sintering depth (layer thickness) as well as the multilayer behaviour. Following the representation of the results are focused on polystyrene powder with the particle size of less than 100  $\mu\text{m}$  having the shape of shavings.

Figure 15 shows the energy density of a single melted track versus hatch distance for two different intensities, respective laser powers ( $d_L$  is 0.35mm). The hatched zones mark the working areas. In respect to the assumptions described above it is clearly to see, that for receiving compact panels an increase in hatching distance is guided by an increase of the required energy density. Regarding the working areas for the two laser powers there is a shift using higher laser power to lower energy densities and smaller areas. This is due to the limited interaction time of laser beam and powder bed.

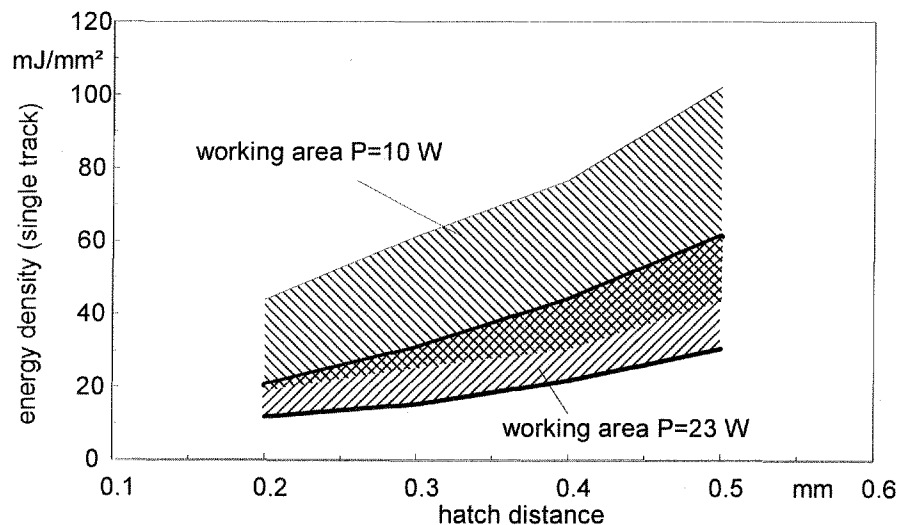


Figure 15: Energy density versus hatch distance for different laser powers.

Within the parameter range various numbers of parts were built using Polystyrene and elastomer modified Polyamid, respectively to their working areas. No surface finishing or infiltration was performed for postprocessing. It was proved that there were no geometric restrictions for complex geometries due to both polymers. (see fig. 16-white parts). The Polystyrene parts showed a porous surface (max. surface roughness of 60 $\mu\text{m}$ ) corresponding to the comparatively big particle size and brittle behaviour while the mechanical behaviour of the PA-Copolymer parts showed their typical properties of 350% elongation at break.

### 3.2 Investment casting via direct burn-out

The Polystyrene parts were embedded in the plaster block moulding and burnt out afterwards completely. Investment casting of aluminum alloy AlSi10Mg and AlSi9Cu3 was performed. Figure 16 shows an overview of some PS and PA-Copolymer parts with the corresponding aluminum casts. The results present, that PS is very suitable for lost pattern/lost mold to be used for unmodified investment casting. No changes in the normal process chain are necessary. The surface roughness of aluminum parts is as high as the corresponding polymer parts.

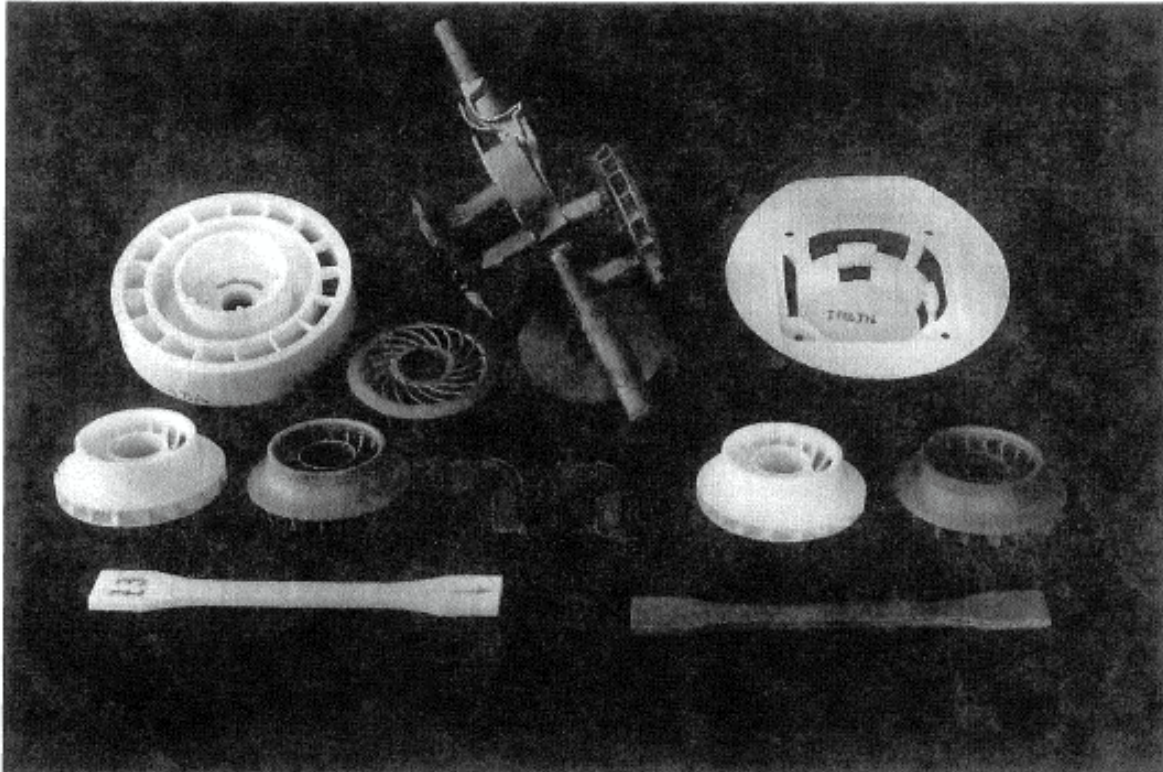


Figure 16: Overview of Polymer parts and corresponding metal parts via investment casting. Bottom: tensile specimen (PS/aluminum); middle: turbine blade housings (left: PA-Copolymer/aluminum, right: PS/aluminum); top: left: turbine (PS); middle: investment casted wax tree (before disassembling); right: loudspeaker housing (PS).

### 4. Acknowledgements

The authors thank the students for their comprehensive work done on parameter optimization and further development of the LAPS-equipment. The research in respect of metal layer powder application is funded by the European Commission (Programme Brite/EuRam).

The authors thank the partners and endorsers of the project. Also Karl-Heinz Schade from Emil Bucher GmbH&Co, Eislungen/Fils (FRG), who has performed the investment castings and prevented us with relevant datas on casting techniques.

## 5. References

- [1] Zong, G.; Wu, Y.; Tran, N.; Lee, I.; Bourell, B.L.; Beaman, J.J.: Direct Selective Sintering of High Temperatur Materials. In: Marcus, H.Z.; Beaman, J.J.; Barlow, J.W.; Bourell, D.L.; Crawford, R.H.(Hrsg.): Solid Freeform Fabrication Proceedings, Austin, USA, August 1992, pp. 72-85.
- [2] Kaysser, W.A.: Sintern mit Zusätzen. Materialkundlich-Technische Reihe 11, Berlin-Stuttgart: Gebrüder Borntraeger, 1992.
- [3] Schatt, W.: Sintervorgänge, Grundlagen. Düsseldorf: VDI-Verlag GmbH, 1992.
- [4] Massalski, T.B.: Binary Alloy Phase Diagrams Vol. I. American Society for Metals, Metals Park, Ohio 44073, 1986. ISBN 0-87170-262-2
- [5] Haag, M: CO<sub>2</sub> Laser Absorption Characteristics of Metal Powders. Institut für Strahlwerkzeuge (IFSW), University of Stuttgart. Diplomarbeit, 1994